Suspension Plasma Spray Fabrication of Nanocrystalline Titania Hollow Microspheres for Photocatalytic Applications

Kun Ren, Yi Liu, Xiaoyan He & Hua Li

Journal of Thermal Spray Technology

ISSN 1059-9630

J Therm Spray Tech
DOI 10.1007/s11666-015-0296-1

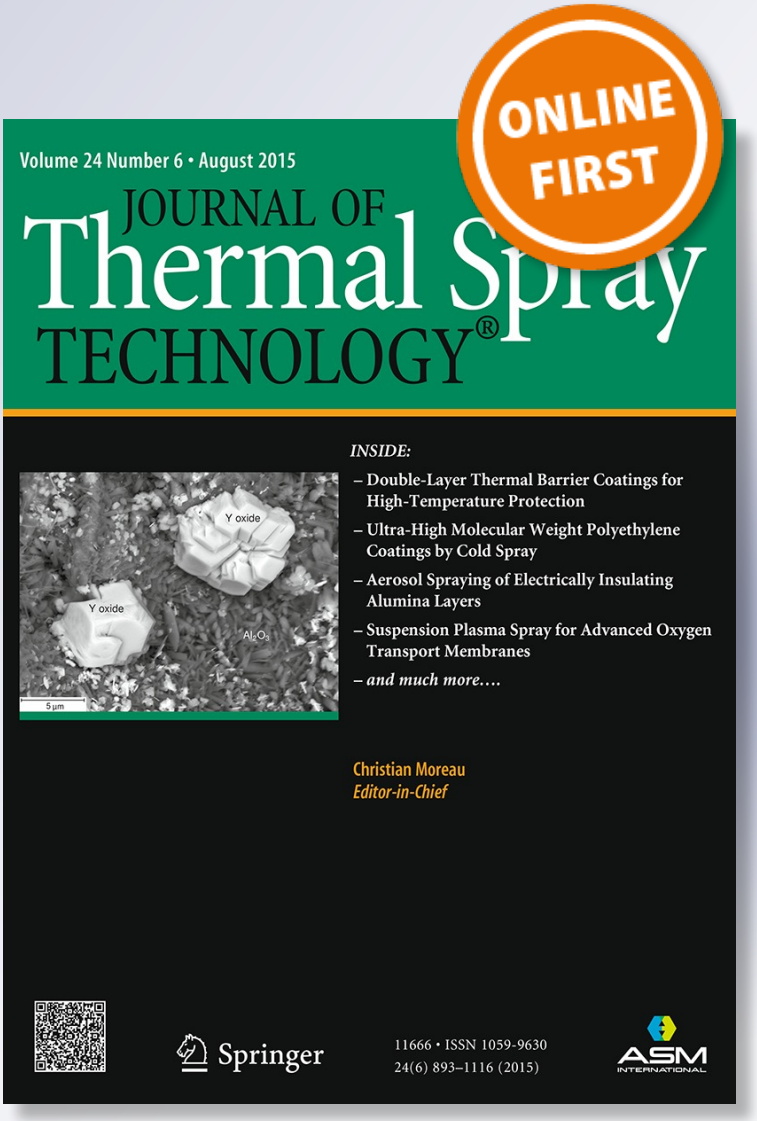

Springer

JTTEE5
DOI: 10.1007/s11666-015-0296-1
1059-9630/$19.00 © ASM International

Suspension Plasma Spray Fabrication of Nanocrystalline Titania Hollow Microspheres for Photocatalytic Applications

Kun Ren, Yi Liu, Xiaoyan He, and Hua Li

(Submitted April 27, 2015; in revised form August 18, 2015)

Hollow inorganic microspheres with controlled internal pores in close-cell configuration are usually constructed by submicron-sized particles. Fast and efficient large-scale production of the microspheres with tunable sizes yet remains challenging. Here, we report a suspension plasma spray route for making hollow microspheres from nano titania particles. The processing permits most nano particles to retain their physiochemical properties in the as-sprayed microspheres. The microspheres have controllable interior cavities and mesoporous shell of 1-3 μm in thickness. Spray parameters and organic content in the starting suspension play the key role in regulating the efficiency of accomplishing the hollow sphere structure. For the ease of collecting the spheres for recycling use, ferriferous oxide particles were used as additives to make Fe_3O_4-TiO_2 hollow magnetic microspheres. The spheres can be easily recycled through external magnetic field collection after each time use. Photocatalytic anti-bacterial activities of the hollow spheres were assessed by examining their capability of degrading methylene blue and sterilizing *Escherichia coli* bacteria. Excellent photocatalytic performances were revealed for the hollow spheres, giving insight into their potential versatile applications.

Keywords hollow spheres, magnetic microspheres, nano titania, photocatalytic performances, suspension plasma spray

1. Introduction

Owing to their high specific surface area, low density, and other excellent performances, inorganic hollow spheres showed great promises for various applications (Ref 1, 2). Hollow spheres are potential candidates for drug delivery (Ref 2, 3), refractory thermal insulation (Ref 4), electrode (Ref 5, 6), and environmental purification (Ref 3, 7-9). The major variables of hollow spheres are essentially sphere size and aspect ratio (the ratio of sphere diameter to wall thickness), which pertain to fabrication techniques (Ref 10, 11). Preparation of hollow particles is usually intrinsically associated with the need of the use of templates (Ref 1, 3, 5, 8, 12-17), through which the particle size can be accurately controlled. This, however, raises the demand for post-treatment to remove the templates, which usually results in insufficient strength of the spheres to maintain the hollow geometry. A variety of fabrication techniques using soft templates or no template, for instance sol-gels/emulsions (Ref 18-21), spray precipitation and spray pyrolysis (Ref 22, 23), and spray drying (Ref 24), were then developed for making particular hollow capsule structure. Among the methods, solution- or colloid-based techniques showed the capability to control the morphology and size of the microspheres, but they are not suitable for mass production due to the disadvantages like relatively complex and time-consuming processing (Ref 25). Fast and cost-effective fabrication of hollow microspheres with adjustable sizes still remains elusive.

Bacterium-related environmental issues, such as the drinking water problem, due to the presence of microorganisms in water have been gaining intensive worldwide concerns. It was reported that about 80-90% of the water-related diseases are caused by contamination with pathogenic microorganisms (Ref 26). To attain clean water, many disinfection processes have been developed, such as ozonation, chlorine dioxide treatment, advanced filtration, and germicidal ultraviolet radiation. Yet, the above traditional methods usually bear high cost, complex treatment, and detrimental byproducts, which in turn restricts their potential applications. Novel water disinfection techniques are, therefore, to be developed. Photocatalysis becomes a viable option by virtue of the use of sunlight to actuate the disinfection process and minimal hazardous disinfection byproducts. Among the possible semiconductor catalysts, titanium dioxide (TiO_2) has been used extensively as photocatalyst to degrade organic compounds and microorganisms for the last 40 years. This is

Kun Ren, Yi Liu, Xiaoyan He, and **Hua Li**, Key Laboratory of Marine Materials and Related Technologies, Zhejiang Key Laboratory of Marine Materials and Protective Technologies, Ningbo Institute of Materials Technology and Engineering, Chinese Academy of Sciences, Ningbo 315201, China. Contact e-mail: lihua@nimte.ac.cn.

Published online: 03 September 2015

attributed to its favorable chemical stability, long durability, nontoxicity, low cost, and recyclable use without substantial loss of catalytic ability (Ref 27, 28). However, separation of the photocatalysts in powder form from the solution following photocatalytic reaction can be very difficult and the tendency of the particles to agglomerate into larger particles effectively reduces the photocatalytic activity (Ref 29). Hollow titania spheres with magnetic feature could be a potential candidate to overcome the problems. Microspheres would not aggregate easily during service, and magnetic separation has been a convenient approach for separating magnetized species easily and thoroughly by a simple magnetic device (Ref 30). To date, many approaches can be used to make titania hollow spheres, for instance hard template method (Ref 31-33), soft template method (Ref 12, 34), or template-free method (Ref 7, 35, 36). However, fabrication of the hollow spheres with appropriate structures is a persistent challenge and the approach used for blending the magnetic materials into titania needs to be explored.

As one of the key surface modification techniques, thermal spray offers the advantages of cost-efficiency, wide selection of coating materials, and easy on-site operation, making it one of the versatile coating techniques. This technique already showed feasibility of fabricating new materials in powder form (Ref 37). Spray techniques are most fitting for large-scale production of big spheres (Ref 38). In this study, we proposed suspension plasma spray processing route for mass production of hollow inorganic microspheres. Nano titania and Fe_3O_4 (100-300 nm) particles were used as the starting feedstock materials. Formation mechanism of the hollow spheres was elucidated and their photocatalytic performances were examined.

2. Materials and Methods

Starting titania suspension was prepared by ultrasonically dispersing 50 g of Degussa TiO_2 (Evonik Degussa P25, 99.5%) in 1 L 50% ethanol solution containing 10 g polyvinylpyrrolidone (PVP) and 5 g polyethylene glycol (PEG). The commercially available P25 titania had the size of ~21 nm in diameter and comprised ~80 wt.% anatase and ~20 wt.% rutile. The suspension was magnetically stirred for 30 min to achieve homogeneous dispersion for further use. The APS-2000K plasma spray system (Beijing Aeronautical Manufacturing Technology Research Institute, China) was employed for fabricating the hollow spheres. The spray conditions are listed in Table 1. For fabricating the Fe_3O_4-TiO_2 hollow magnetic microspheres, 19 g P25 and 1 g magnetic ferriferrous oxide powder (100-300 nm in diameter, Aladin Reagent Corporation, China) were ultrasonically dispersed and mechanically stirred for 60 min in a 500 ml 20 vol.% alcoholic solution containing 4 g PVP and 1 g PEG. During the spraying, the slurry was pumped at a speed of 45 ml/min into the downstream of the plasma arc 2 mm away from the gun exit. The pumping was carried out using a peristaltic pump and home-made injection system. The slurry was propelled downwardly into the arc followed by atomization and evaporation of the water in the particles. The hollow spheres were collected in air by a 316 L container. Further calcination was carried out at 500°C for 2 h to remove the remaining organics in the as-sprayed spheres.

Table 1 Plasma spray conditions for fabricating the hollow spheres

Parameter	Value
Internal diameter of anode nozzle	7.5 mm
Position of the injector	2 mm away from gun exit
Ar	40 slm, 0.5 MPa
H_2	0.3 MPa
Power	14, 20, 25, 30, 36 kW

Phase composition of the samples was analyzed by x-ray diffraction (XRD, D8 Advance, Bruker AXS, Germany) using CuKα radiation operated at 40 kV and 40 mA. The goniometer was set at a scan rate of 0.02°/s over a 2θ range of 10°-90°. Morphology of the samples was characterized using field emission scanning electron microscopy (FESEM, FEI Quanta FEG250 and FEI Quanta FEG S4800) equipped with energy dispersive spectrometer. Particle size distribution was measured by a laser granulometer (Microtrac S3500 Particle Size Analyzer, USA). Fourier transform infrared spectroscopy (FTIR, Nicolet 6700, Thermo Fisher Scientific, USA) was also used for characterization of the samples. The infrared spectrum with a resolution of 4 cm and the scan number of 8 were adopted with a spectral region from 400 to 4000/cm. Magnetic properties of the spheres were measured by acquiring their saturation magnetization curves at room temperature via a vibrating sample magnetometer (VSM, Lakeshore 7410, USA).

For assessment of the photocatalytic activities of the hollow spheres, photodegradation by the spheres of methylene blue (MB, Aladdin Reagent Corporation, China) and extinguishment of gram-negative *Escherichia coli* (*E. coli*, ATCC25922) bacteria were examined. For the MB degradation testing, 5 mg sample powder was added into Ø9 cm Petri culture dish containing 25 ml MB solution (5 ppm) and then mechanical dispersion was conducted by magnetic stirring for 1 h in the dark to ensure adsorption/desorption equilibrium before irradiation. The irradiation was carried out using natural sunlight illumination. Variations of MB concentration were analyzed by reading the peak absorption of MB at 664 nm using a UV-Vis spectrophotometer (Lambda 950, Perkin-Elmer, USA). Further photocatalytic activity of the hollow spheres against pathogenic organisms was examined by sterilization testing using *E. coli* bacteria. The bacteria were cultivated in a shaker operated at 120 rpm for 24 h at 30 °C. They were harvested by centrifugation at 2500 rpm and washed three times with 0.85% NaCl solution before being resuspended at a concentration of 5×10^7 CFU/ml in 0.85% NaCl solution. CFU (colony forming units) refers to the number of living bacteria in the

suspension. The concentration of the powder used was 1 g/L, and the powder was dispersed by sonication for 30 min in 0.85% NaCl solution. Afterwards 15 ml of the bacterial suspension and 15 ml of powder suspension was added into a Petri dish. Irradiation was produced by a 15 W UV lamp (PHILIPS, TLD15 W BL) with the typical wavelength of 365 nm and the distance between the UV light source and the samples was 15 cm. For qualitative examination of anti-bacterial activity of the samples, 2 µl of each sample after the UV illumination was dibbled on the designated spot of a nutrient agar plate. For quantitative investigation, 100 µl of each sample with different testing conditions was spread on separate nutrient agar plate. The plates were incubated for 24 h at 37 °C in an incubator before examining the bacterial colonies.

3. Results and Discussion

It was realized in this study that plasma power does not remarkably affect the sphericity of the spheres, instead it crucially affects the sizes of the hollow microspheres (Fig. 1a and 2). Higher plasma power results in smoother surfaces and larger diameter. PVP decides predominately the sphericity of the as-sprayed particles (Fig. 1b). It is noted that the content of PVP plays a significant role in affecting the formation of hollow microspheres and it acts as a binder facilitating pelletization during the spraying. Other spray parameters, for example feeding rate of the suspension, gas flow rate, etc., showed certain influence on geometrical morphology and chemistry of the hollow microspheres. Yet they are not as important as spray power and content of PVP in the suspension. It is reasonable that higher spray power brings about higher droplet temperature and higher diffusion rate of the organics, in turn facilitating the droplets keeping their microspherical shape (Ref 39). In addition, higher temperature results in more gas generated, giving rise to higher interior pressure so that the sphere is further dilated. However, it was noted that further increased plasma power would promote grain growth and anatase-rutile transformation,

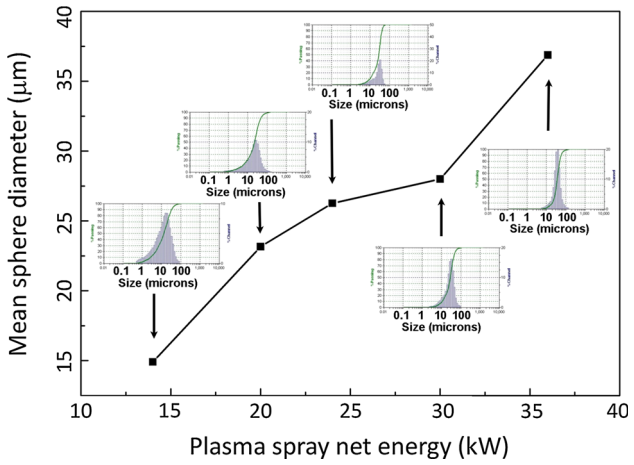

Fig. 2 Influence of plasma spray power on particle sizes of the hollow spheres

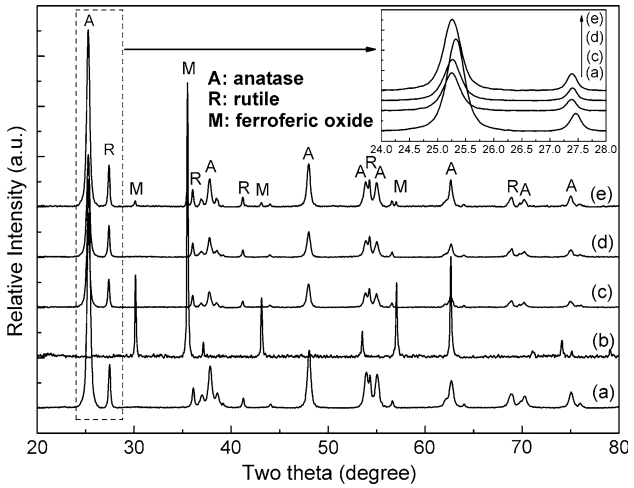

Fig. 3 XRD patterns of (a) the starting P25 nano powder, (b) the starting Fe_3O_4 nano powder, (c) the as-sprayed TiO_2 hollow spheres, (d) the post-spray calcined TiO_2 hollow spheres, and (e) the TiO_2-Fe_3O_4 hollow microspheres

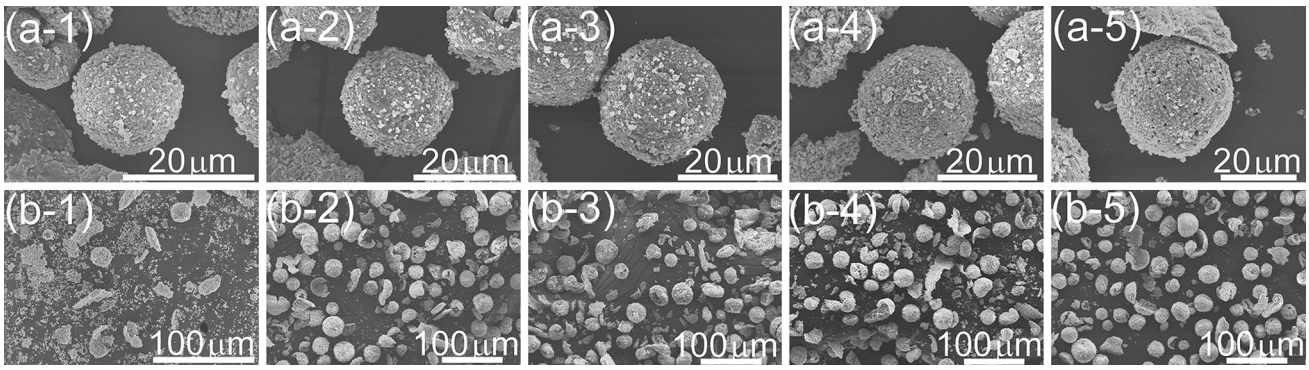

Fig. 1 Typical SEM images showing the effect of spray power (a) and content of PVP in the starting suspension (b) on the sizes and the morphology of the hollow spheres, (a-1) net energy of 14 kW, (a-2) net energy of 20 kW, (a-3) net energy of 25 kW, (a-4) net energy of 30 kW, (a-5) net energy of 36 kW; (b-1) PVP content of 0.25%, (b-2) PVP content of 0.5%, (b-3) PVP content of 1.0%, (b-4) PVP content of 1.5%, (b-5) PVP content of 2.0%

which might greatly deteriorate the performances of the spheres. PEG was used as the surfactant to disperse TiO_2 nanoparticles uniformly in the suspension. The binder does not show marked effect on the sphericity of the spheres. PVP as a stabilizer can prevent the nano TiO_2 particles from aggregating and sedimenting in the starting suspension. Known as a capping reagent for micron-sized particles, PVP has a strong stickiness. PVP could electrostatically adhere strongly to the surface of TiO_2 nanoparticle in ethanol solution (Ref 40).

Optimization of the spray parameters suggests that the spray power of 25 kW is appropriate for constructing the hollow spheres. In addition, when the mass ratio of TiO_2/PVP is higher than 20, almost no microspheres were made. As the mass ratio is lower than 1, it is difficult for the particles to sustain spherical shape, presumably because the high viscosity of the suspension impairs the surface tension of the atomized droplets. The optimum mass ratio of TiO_2/PVP is 2.5-5 for accomplishing good sphericity of the hollow spheres. The spray power of 25 kW and TiO_2/PVP ratio of 5 were then chosen for fabrication of the spheres.

Almost identical XRD peaks for the original, the as-sprayed, and the post-spray calcined powder have been detected (Fig. 3). Trace of the peaks for rutile is recognized in the as-sprayed powder. Based on the quantification formula calculated from the relative intensity of the major XRD peaks, $X_R = (1 + 0.884 I_A/I_R)^{-1}$ (Ref 41), where X_R is the weight fraction of rutile and I_A and I_R are the XRD peak intensity of the (101) peak of anatase and

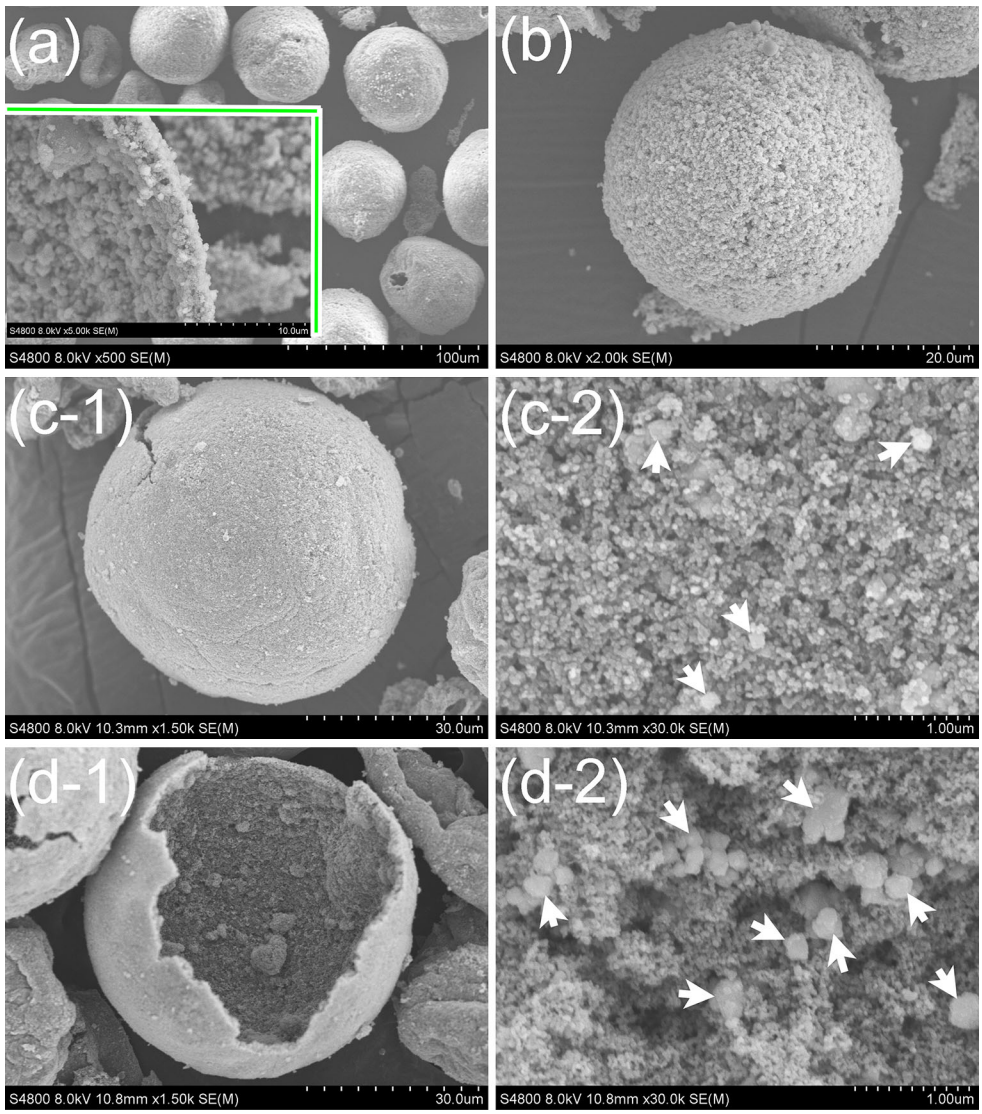

Fig. 4 FESEM views of (a) the as-sprayed pure TiO_2 hollow microspheres, (b) the post-spray calcined TiO_2 hollow microspheres, (c) the surface views of an intact calcined Fe_3O_4-TiO_2 hollow sphere, and (d) the views from a crushed Fe_3O_4-TiO_2 hollow microspheres showing the wall thickness of 1-3 μm. The inset in (a) is enlarged view of a crushed TiO_2 hollow sphere showing well-retained nano titania. The images (c-2, d-2) are magnified views of selected areas of (c-1) and (d-2), respectively, showing unique presence of Fe_3O_4 particles in both the outside surface and the inside surface of the spheres. The arrows point to Fe_3O_4 particles

the (110) peak of rutile, respectively. ~20% rutile is detected in the titania hollow spheres (Fig. 3c versus a). No remarkable transformation of anatase to rutile is indicated. This nevertheless suggests moderate heating experienced by the particles during the spraying. Further calcination treatment did not cause increase in the content of rutile in the hollow spheres, which is not surprising since the sintering temperature is much lower than the value required for anatase to rutile transformation. For the spheres with Fe_3O_4 addition, trace of the magnetic ferrous ferric oxide in the composites is suggested by its weak XRD peaks (Fig. 3e), even though the dosage of the oxide is low. No spectra for ferric oxide or iron titanium oxide can be seen, suggesting negligible phase changes of Fe_3O_4 and mutual reaction between titania and Fe_3O_4 during the spraying. The spray processing permits most nano particles to retain their physiochemical properties in the resultant microspheres.

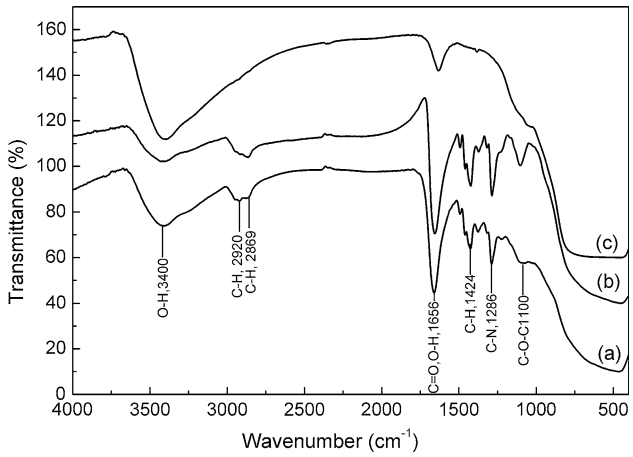

Fig. 5 FTIRs spectra of (a) the as-sprayed TiO_2 hollow microspheres, (b) the as-sprayed TiO_2-Fe_3O_4 hollow microspheres, and (c) the post-spray calcined TiO_2-Fe_3O_4 hollow microspheres

Nanostructured TiO_2 microspheres exhibit the sizes of 15-40 μm in diameter (Fig. 4a) and a thin wall (inset in Fig. 4a). It is noted that certain amount of the organic binder was retained in the as-sprayed spheres (as evidenced by their IR spectrum shown in Fig. 5a), which is due to the insufficient heating of the particles during the spraying. Therefore, post-spray calcination at 500 °C for 2 h is necessary for effectively removing the organics in the particles. Compared to the as-sprayed spheres, the calcination processing did not trigger changes in either contours or physical features (Fig. 4b). In addition, as noticed from both the topographical and crushed views of the Fe_3O_4-containing particles (Fig. 4c, d), the bigger magnetite particles are clearly seen on both the outside surface and the inside surface of the spheres, which are dispersed in the composite structure. The interior cavities with a mesoporous shell of 1-3 μm in thickness are seen from the crushed spheres (Fig. 4d-1 and the inset in Fig. 4a). The thickness of the wall is uniform for each hollow sphere. It has been realized that spray parameters and organic content in the starting suspension play the key role in deciding the efficiency of accomplishing the hollow sphere structure.

Formation of the hollow spheres is likely resulted from effective water evaporation and gas escape during the heating of the droplets fed into the plasma torch. In the initial stage, the suspension droplets injected into the torch are usually atomized into small droplets. Heating of the droplets in turn leads to formation of the spheres in virtue of surface tension from water evaporation and decomposition of the organics. Solidified surface of the droplets would shape a spherical shell with a specific size on account of plasma spheroidization (Ref 42-44) and surface tension. There are essentially two processes occurring simultaneously for the particles flying in the torch, heat, and mass transfer. According to this theory, the internal solid-liquid mixture in the droplet would transfer to the surface and heat will transfer inward during the spraying. It is usual that substances transfer to the

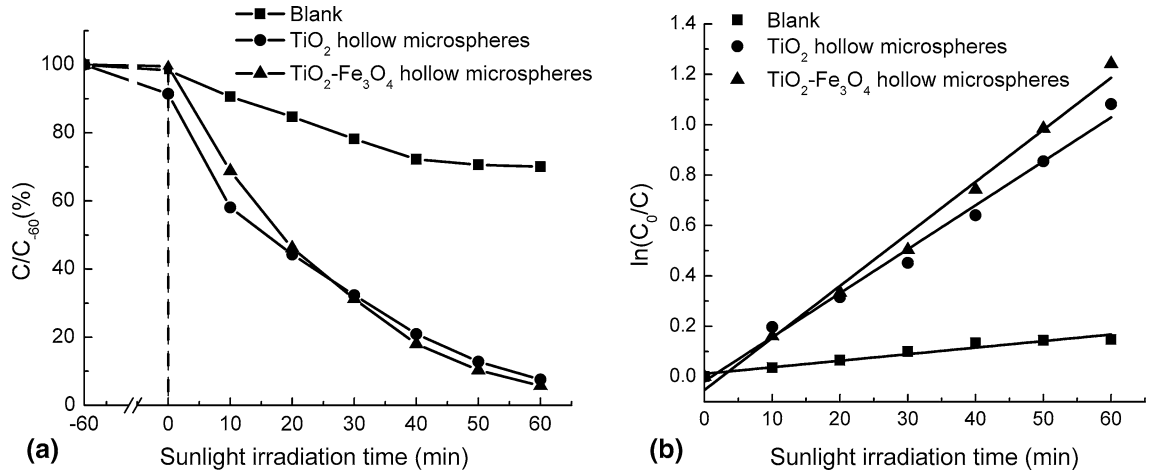

Fig. 6 Photocatalytic activity assessment of the powder samples under sunlight irradiation, (a) variation of MB concentration vs. sunlight illumination time, and (b) $\ln(C_0/C)$ against sunlight irradiation time in the presence or absence of the hollow microspheres

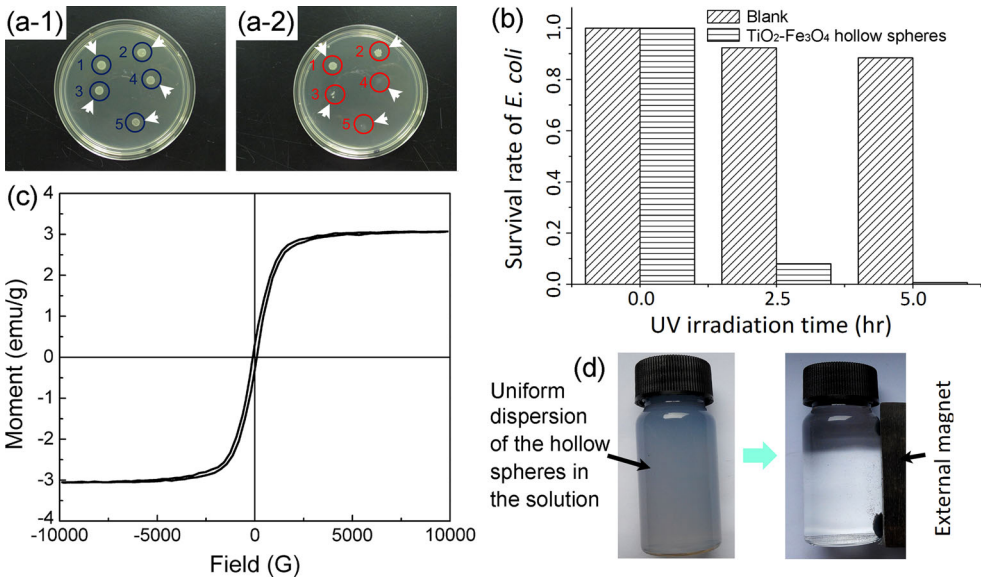

Fig. 7 (a, b) Photocatalytic sterilization results of the TiO_2-Fe_3O_4 hollow spheres against *E. coli*, (a-1) digital photos of *E. coli* colonies in the blank Petri dish after 1, 2, 3, 4, and 5 h of UV irradiation, and (a-2) digital photos of *E. coli* colonies in the Petri dish after 1 h of UV irradiation (#1), after 2 h of irradiation (#2), after 3 h of irradiation (#3), after 4 h of irradiation (#4), and after 5 h of irradiation (#5), (b) statistical results of the photocatalytic sterilization efficiencies of the samples against *E. coli* vs. UV irradiation time, (c) the saturation magnetization curve acquired at room temperature for the TiO_2-5wt.%Fe_3O_4 hollow spheres, and (d) the micron-sized hollow spheres suspended in the solution can be easily collected by external magnetic field

surface and a hole results in the center. In addition, the steam and gas generated from decomposition of the organics opts to gather and expand. Once heating begins, they can escape through the channels between unmelted particles. After the shell has reached a certain thickness or molten organics have sealed the channels, the melting front pushes the gases toward the center owing to the high surface tension of the molten particles (Ref 45). Those bubble holes assemble and engender a high pressure, eventually puffing the hole forming into a sphere (Ref 24, 46). In the cases that the shell cannot bear the high pressure, the sphere would crack into a lot of fragments. These can explain the significant influence of the key spray parameters on the formation of the hollow spheres. Controlling the parameters appropriately by, for example, changing the percentage of PVP and adjusting the plasma power, could improve the balling rate and lessen the breakage rate.

FTIR analyses of the spheres with/without the post-spray calcination suggest clearly the presence/absence of the organic binder in the spheres (Fig. 5). The broad peaks located at 3400 and 1660/cm are attributed to water and hydroxyl groups adsorbed on titania surface (Ref 47). Presence of the residual organic species (PVP/PEG in this case) in the as-sprayed spheres is evidenced by the appearance of the peaks at 1100, 1288, 1426, and 1660/cm. The IR peaks at 2920 and 2869/cm are assigned to C-H stretching vibrations of residual organics (Ref 48). The broad band located at 800-400/cm refers to Fe-O, Ti-O, and Ti-O-Ti skeletal frequency region (Ref 47, 49). Being consistent with the SEM observation, the IR spectrum of the calcined spheres (Fig. 5c) suggests clearly the entire removal of the organic binder after the calcination treatment. Suspension plasma spray followed by sintering calcination is, therefore, an appropriate route for mass production of nanostructured hollow titania microspheres with predominate component of anatase.

UV-Vis spectra of the hollow microspheres already showed remarkable absorbance in the visible range (curves not shown). The photocatalytic activities of the hollow microspheres were then further assessed by photodegradation of MB under sunlight illumination (Fig. 6). C_{-60} is the MB concentration measured 60 min before the illumination. It is noted that under the sunlight irradiation, both the titania and the TiO_2-Fe_3O_4 hollow spheres already caused the decrease of MB concentration by 92.4% after only an hour exposure (Fig. 6a), while the control sample only shows the drop of MB concentration by ~30%. The photocatalytic degradation usually follows Langmuir-Hinshelwood first-order kinetic model which is usually applied to low concentrations (Ref 50, 51). From the model, the equation, $\ln(C_0/C) = k_{app} \times t$, can be obtained, where C is the MB concentration, C_0 is the initial MB concentration, t is reaction time, k_{app} is the apparent rate constant representing photocatalytic degradation rate. The variations in $\ln(C_0/C)$ as a function of sunlight irradiation time are shown in Fig. 5b. The apparent rate constants are 0.017, 0.020, and 0.002/min for the TiO_2 hollow spheres, the TiO_2-5wt.%Fe_3O_4 hollow spheres, and the control, respectively. This suggests strong photocatalytic performances of the hollow spheres even under sunlight illumination. It was reported that P25 possesses weak photocatalytic activity under visible light irradiation (Ref 52, 53). The excellent photodegradation performance of the thermal sprayed hollow microspheres might be ascribed to possible carbon doping and adsorption of

remnant free carbon. The carbon doping could be indicated by the slight shift of the main XRD peak for anatase after the spray processing, which can be clearly seen from the enlarged view of the peak (inset in Fig. 3). Yet this speculation needs further experimental evidence, and systematical characterization is required to elucidate the promising photocatalytic activity of the hollow spheres.

Further photocatalytic activity of the Fe_3O_4-containing hollow spheres against *E. coli* bacteria was examined (Fig. 7a, b). Excellent photocatalytic sterilization performances were revealed for the TiO_2-Fe_3O_4 hollow spheres. As the control for the testing against *E. coli*, the blank sample exhibited undetectable photocatalytic sterilization even after 5 h of UV irradiation, as evidenced by the good shape of the bacterial colony in the Petri dish (Fig. 7a-1). In contrast, for the spheres samples, the disappearance of the bacterial colonies (#4 and #5) in the Petri dish (Fig. 7a-2) suggests that most of the bacteria were killed by the hollow microspheres after 4 h of UV irradiation. 2 h exposure to UV already resulted in marked loss of bacteria (colony #2 in Fig. 7a-2). This implies the excellent photocatalytic sterilization performance of the magnetic spheres. To more clearly assess the bacteria-killing capability of the powder samples, the bacterial survival ratio versus irradiation time was statistically measured (Fig. 7b). After 5 h of UV irradiation, ~99% bacteria were already killed by the spheres. Therefore, it is clear that the addition of Fe_3O_4 does not deteriorate the photocatalytic performances of the TiO_2 hollow spheres. More importantly, the TiO_2-Fe_3O_4 hollow spheres showed excellent magnetic properties as suggested by their saturation magnetization curve acquired at room temperature (Fig. 7c). The hysteresis loop testing result indicates that the as-sprayed powder could be considered as ferrimagnet. The saturation magnetization value of the Fe_3O_4-5wt.%TiO_2 hollow spheres is 3.1 emu/g. And the residual magnetization and coercivity exhibit small values. In fact, after extinguishing the *E. coli* bacteria in water, the micron-sized spheres can be easily collected by external magnetic field for further use (Fig. 7d). These magnetic hollow spheres have bright prospects for disinfecting the water contaminated with pathogenic microorganisms. Part of our ongoing efforts is devoted to further clarifying the possibility of extending the applications of the anti-bacterial magnetic hollow spheres.

4. Conclusions

Nanostructured TiO_2 hollow microspheres with tunable diameter of 15-40 μm and mesoporous shell of 1-3 μm in thickness were successfully fabricated by suspension plasma spray. Physicochemical features of the nano titania are mostly retained after the fabrication. The physical features of the spheres, i.e., size, shell thickness, etc., are tailorable by adjusting plasma power, content of the organic binder, and concentration of the suspension. The hollow spheres showed excellent photocatalytic performances, and the addition of magnetic Fe_3O_4 particles does not affect the spray processing and photocatalytic activity of the titania-based hollow spheres. It instead offers the ease of collecting the spheres by applying external magnetic field after each time it is used for photocatalytic disinfection. The suspension thermal spray route proposed in this research for fabricating nano titania and TiO_2-Fe_3O_4 hollow microspheres opens a new window for cost-effective mass production of nanostructured hollow spheres using multiple materials with exceptional properties for various applications.

Acknowledgments

This research was supported by National Natural Science Foundation of China (Grant # 41476064 and 31271017) and Ningbo Municipal Natural Science Foundation (Grant # 2013A610140 and 2013A610150).

References

1. T. Nomura, Y. Morimoto, M. Ishikawa, H. Tokumoto, and Y. Konishi, Synthesis of Hollow Silica Microparticles from Bacterial Templates, *Adv. Powder Technol.*, 2010, **21**(2), p 218-222
2. G.X. Yang, S.L. Gai, F.Y. Qu, and P.P. Yang, SiO_2@YBO_3: Eu^{3+} Hollow Mesoporous Spheres for Drug Delivery Vehicle, *ACS Appl. Mater. Interfaces*, 2013, **5**(12), p 5788-5796
3. N.H. Ran, L. Yuliati, S.L. Lee, T.M. Mahlia, and H. Nur, Liquid-Gas Boundary Catalysis by Using Gold/Polystyrene-Coated Hollow Titania, *J. Colloid Interface Sci.*, 2013, **394**, p 490-497
4. L.I.C. Sandberg, T. Gao, B.P. Jelle, and A. Gustavsen, Synthesis of Hollow Silica Nanospheres by Sacrificial Polystyrene Templates for Thermal Insulation Applications, *Adv. Mater. Sci. Eng.*, 2013, **2013**, p 1-6
5. L. Xiao, M.L. Cao, D.D. Mei, Y.L. Guo, L.F. Yao, D.Y. Qu, and B.H. Deng, Preparation and Electrochemical Lithium Storage Features of TiO_2 Hollow Spheres, *J. Power Sources*, 2013, **238**, p 197-202
6. Y. Li, H. Liu, F.J. Liu, C.R. Li, B.Y. Chen, and W.J. Dong, A Simple Approach to Porous Low-Temperature-Sintering $BaTiO_3$, *Sci. China Chem.*, 2012, **55**(9), p 1765-1769
7. J. Yu, S. Liu, and H. Yu, Microstructures and Photoactivity of Mesoporous Anatase Hollow Microspheres Fabricated by Fluoride-Mediated Self-Transformation, *J. Catal.*, 2007, **249**(1), p 59-66
8. A. Syoufian and K. Nakashima, Degradation of Methylene Blue in Aqueous Dispersion of Hollow Titania Photocatalyst: Study of Reaction Enhancement by Various Electron Scavengers, *J. Colloid Interface Sci.*, 2008, **317**(2), p 507-512
9. K.Z. Lv, J. Li, X.X. Qing, W.Z. Li, and Q.Y. Chen, Synthesis and Photo-Degradation Application of WO_3/TiO_2 Hollow Spheres, *J. Hazard. Mater.*, 2011, **189**(1-2), p 329-335
10. J. Bertling, J. Blömer, and R. Kümmel, Hollow Microspheres, *Chem. Eng. Technol.*, 2004, **27**(8), p 829-837
11. M. Scheffler and P. Colombo, *Cellular Ceramics: Structure, Manufacturing, Properties and Applications*, Wiley, Chichester, 2006
12. T.Z. Ren, Z.Y. Yuan, and B.L. Su, Surfactant-Assisted Preparation of Hollow Microspheres of Mesoporous TiO_2, *Chem. Phys. Lett.*, 2003, **374**(1-2), p 170-175
13. T. Nomura, Y. Morimoto, H. Tokumoto, and Y. Konishi, Fabrication of Silica Hollow Particles Using *Escherichia coli* as a Template, *Mater. Lett.*, 2008, **62**(21), p 3727-3729
14. H.R. Kim, Y. Eom, T.G. Lee, and Y.-G. Shul, Preparation and Photocatalytic Properties of Cr/Ti Hollow Spheres, *Mater. Chem. Phys.*, 2008, **108**(1), p 154-159

15. S. Dadgostar, F. Tajabadi, and N. Taghavinia, Mesoporous Submicrometer TiO_2 Hollow Spheres as Scatterers in Dye-Sensitized Solar Cells, *ACS Appl. Mater. Interfaces*, 2012, **4**(6), p 2964-2968
16. J. Chattopadhyay, H.R. Kim, S.B. Moon, and D. Pak, Performance of Tin Doped Titania Hollow Spheres as Electrocatalysts for Hydrogen and Oxygen Production in Water Electrolysis, *Int. J. Hydrog. Energy*, 2008, **33**(13), p 3270-3280
17. Y. Ao, J. Xu, D. Fu, and C. Yuan, A Simple Method for the Preparation of Titania Hollow Sphere, *Catal. Commun.*, 2008, **9**(15), p 2574-2577
18. Y. Wang, A. Zhou, and Z. Yang, Preparation of Hollow TiO_2 Microspheres by the Reverse Microemulsions, *Mater. Lett.*, 2008, **62**(12-13), p 1930-1932
19. H. Groger, C. Kind, P. Leidinger, M. Roming, and C. Feldmann, Nanoscale Hollow Spheres: Microemulsion-Based Synthesis, Structural Characterization and Container-Type Functionality, *Materials*, 2010, **3**(8), p 4355-4386
20. C. Zurmuhl, R. Popescu, D. Gerthsen, and C. Feldmann, Microemulsion-Based Synthesis of Nanoscale TiO_2 Hollow Spheres, *Solid State Sci.*, 2011, **13**(8), p 1505-1509
21. Y.R. Bak, G.O. Kim, M.J. Hwang, K.K. Cho, K.W. Kim, and K.S. Ryu, Fabrication and Performance of Nanoporous TiO_2/SnO_2 Electrodes with a Half Hollow Sphere Structure for Dye Sensitized Solar Cells, *J. Sol-Gel Sci. Technol.*, 2011, **58**(2), p 518-523
22. B. Peng, M. Chen, S. Zhou, L. Wu, and X. Ma, Fabrication of Hollow Silica Spheres Using Droplet Templates Derived From a Miniemulsion Technique, *J. Colloid Interface Sci.*, 2008, **321**(1), p 67-73
23. S. Nagamine, A. Sugioka, and Y. Konishi, Preparation of TiO_2 Hollow Microparticles by Spraying Water Droplets into an Organic Solution of Titanium Tetraisopropoxide, *Mater. Lett.*, 2007, **61**(2), p 444-447
24. M. Iida, T. Sasaki, and M. Watanabe, Titanium Dioxide Hollow Microspheres with an Extremely Thin Shell, *Chem. Mater.*, 1998, **10**(12), p 3780-3782
25. A.J. Wang, Y.P. Lu, and R.X. Sun, Recent Progress on the Fabrication of Hollow Microspheres, *Mater. Sci. Eng. A*, 2007, **460**, p 1-6
26. K. Backhaus, J. Marugan, R. van Grieken, and C. Sordo, Photocatalytic Inactivation of *E. Faecalis* in Secondary Wastewater Plant Effluents, *Water Sci. Technol.*, 2010, **61**(9), p 2355-2361
27. J. Gamage and Z. Zhang, Applications of Photocatalytic Disinfection, *Int. J. Photoenergy*, 2010, **2010**, p 1-11
28. K. Nakata and A. Fujishima, TiO_2 Photocatalysis: Design and Applications, *J. Photochem. Photobiol. C*, 2012, **13**(3), p 169-189
29. F. Ye and A. Ohmori, The Photocatalytic Activity and Photo-Absorption of Plasma Sprayed TiO_2-Fe_3O_4 Binary Oxide Coatings, *Surf. Coat. Technnol.*, 2002, **160**(1), p 62-67
30. M. Shokouhimehr, Y. Piao, J. Kim, Y. Jang, and T. Hyeon, A Magnetically Recyclable Nanocomposite Catalyst for Olefin Epoxidation, *Angew. Chem.*, 2007, **119**(37), p 7169-7173
31. A. Imhof, Preparation and Characterization of Titania-Coated Polystyrene Spheres and Hollow Titania Shells, *Langmuir*, 2001, **17**(12), p 3579-3585
32. X.X. Li, Y.J. Xiong, Z.Q. Li, and Y. Xie, Large-Scale Fabrication of TiO_2 Hierarchical Hollow Spheres, *Inorg. Chem.*, 2006, **45**(9), p 3493-3495
33. J. Yu, W. Liu, and H. Yu, A One-Pot Approach to Hierarchically Nanoporous Titania Hollow Microspheres with High Photocatalytic Activity, *Cryst. Growth Des.*, 2008, **8**(3), p 930-934
34. S. Xuan, W. Jiang, X. Gong, Y. Hu, and Z. Chen, Magnetically Separable Fe_3O_4/TiO_2 Hollow Spheres: Fabrication and Photocatalytic Activity, *J. Phys. Chem. C*, 2009, **113**(2), p 553-558
35. T. Nakashima and N. Kimizuka, Interfacial Synthesis of Hollow Tio_2 Microspheres in Ionic Liquids, *J. Am. Chem. Soc.*, 2003, **125**(21), p 6386-6387
36. H. Li, Z. Bian, J. Zhu, D. Zhang, G. Li, Y. Huo, H. Li, and Y. Lu, Mesoporous Titania Spheres with Tunable Chamber Structure and Enhanced Photocatalytic Activity, *J. Am. Chem. Soc.*, 2007, **129**(27), p 8406-8407
37. O.P. Solonenko, I.P. Gulyaev, and A.V. Smirnov, Thermal Plasma Processes for Production of Hollow Spherical Powders: Theory and Experiment, *J. Therm. Sci. Tech.*, 2011, **6**(2), p 219-234
38. R.K. Singh, A. Garg, R. Bandyopadhyaya, and B.K. Mishra, Density Fractionated Hollow Silica Microspheres with High-Yield by Non-Polymeric Sol-Gel/Emulsion Route, *Colloids Surf. A*, 2007, **310**(1-3), p 39-45
39. Y. Huang, Z. Ai, W. Ho, M. Chen, and S. Lee, Ultrasonic Spray Pyrolysis Synthesis of Porous Bi_2WO_6 Microspheres and Their Visible-Light-Induced Photocatalytic Removal of NO, *J. Phys. Chem. C*, 2010, **114**(14), p 6342-6349
40. T. Thirugnanam, Effect of Polymers (PEG and PVP) on Sol-Gel Synthesis of Microsized Zinc Oxide, *J. Nanomater.*, 2013, **2013**, p 43
41. R.A. Spurr and H. Myers, Quantitative Analysis of Anatase-Rutile Mixtures with an x-Ray Diffractometer, *Anal. Chem.*, 1957, **29**(5), p 760-762
42. J.S. O'Dell, E.C. Schofield, T.N. McKechnie, and A. Fulmer, Plasma Alloying and Spheroidization Process and Development, *J. Mater. Eng. Perform.*, 2004, **13**(4), p 461-467
43. J. Xu, K. Khor, Y. Gu, R. Kumar, and P. Cheang, Radio Frequency (RF) Plasma Spheroidized HA Powders: Powder Characterization and Spark Plasma Sintering Behavior, *Biomaterials*, 2005, **26**(15), p 2197-2207
44. Z. Károly and J. Szépvölgyi, Plasma Spheroidization of Ceramic Particles, *Chem. Eng. Proc.*, 2005, **44**(2), p 221-224
45. Z. Károly and J. Szépvölgyi, Hollow Alumina Microspheres Prepared by RF Thermal Plasma, *Powder Technol.*, 2003, **132**(2), p 211-215
46. G. Pravdic and M. Gani, The Formation of Hollow Spherical Ceramic Oxide Particles in a DC Plasma, *J. Mater. Sci.*, 1996, **31**(13), p 3487-3495
47. G.J. Soler-Illia, A. Louis, and C. Sanchez, Synthesis and Characterization of Mesostructured Titania-Based Materials through Evaporation-Induced Self-assembly, *Chem. Mater.*, 2002, **14**(2), p 750-759
48. B. Rajamannan, S. Mugundan, G. Viruthagiri, P. Praveen, and N. Shanmugam, Linear and Nonlinear Optical Studies of Bare and Copper Doped TiO_2 Nanoparticles via Sol Gel Technique, *Spectrochim. Acta A*, 2014, **118**, p 651-656
49. A.M. Peiró, J. Peral, C. Domingo, X. Domènech, and J.A. Ayllón, Low-Temperature Deposition of TiO_2 Thin Films with Photocatalytic Activity from Colloidal Anatase Aqueous Solutions, *Chem. Mater.*, 2001, **13**(8), p 2567-2573
50. J.J. Xu, M.D. Chen, and D.G. Fu, Study on Highly Visible Light Active Bi-doped TiO_2 Composite Hollow Sphere, *Appl. Surf. Sci.*, 2011, **257**(17), p 7381-7386
51. Y.H. Ao, J.J. Xu, D.G. Fu, and C.W. Yuan, A Simple Method to Prepare N-Doped Titania Hollow Spheres with High Photocatalytic Activity Under Visible Light, *J. Hazard. Mater.*, 2009, **167**(1-3), p 413-417
52. H. Zhang, X. Lv, Y. Li, Y. Wang, and J. Li, P25-Graphene Composite as a High Performance Photocatalyst, *ACS Nano*, 2010, **4**(1), p 380-386
53. J.W. Shi, J.W. Chen, H.J. Cui, M.L. Fu, H.Y. Luo, B. Xu, and Z.L. Ye, One Template Approach to Synthesize C-Doped Titania Hollow Spheres with High Visible-Light Photocatalytic Activity, *Chem. Eng. J.*, 2012, **195**, p 226-232